Available online at www.sciencedirect.com
SCIENCE DIRECT
Polymer 46 (2005) 137–146
polymer
www.elsevier.com/locate/polymer

New water soluble azobenzene-containing diblock copolymers: synthesis and aggregation behavior

P. Ravi[a], S.L. Sin[b], L.H. Gan[b,*], Y.Y. Gan[b], K.C. Tam[a], X.L. Xia[b,c], X. Hu[c]

[a]*Singapore-MIT alliance, School of Mechanical and Production Engineering, Nanyang Technological University, 1 Nanyang Walk, Singapore, Singapore 637616*
[b]*Natural Sciences, National Institute of Education, Nanyang Technological University, 1 Nanyang Walk, Singapore, Singapore 637616*
[c]*School of Materials Engineering, Nanyang Technological University, 1 Nanyang Walk, Singapore, Singapore 637616*

Received 19 July 2004; received in revised form 29 October 2004; accepted 8 November 2004
Available online 23 November 2004

Abstract

Homopolymers of azobenzene (azo) methacrylates with different substituents and their diblock copolymers with poly(2-(dimethylamino)ethyl methacrylate p(DMAEMA) were synthesized via atom transfer radical polymerization (ATRP). Controlled/'living' ATRP of azo methacrylates were achieved up to ~50% conversion, after which deviation occurred. It was found that the copolymerization rate of 6-[4-phenylazo]phenoxy]hexylmethacrylate (PPHM) from p(DMAEMA) macroinitiator was almost identical to that for the homopolymerization of PPHM monomer, with $k_{app} \sim 0.0078\ min^{-1}$. For the copolymerizations, almost complete incorporation of the azo methacrylate monomers could be obtained with low molecular weight macroinitiator (PDMAEMA)-Cl, whereas macroinitiators of long chain length did not give full conversion, most likely due to chain floding and steric hindrance caused by the bulk azo monomers. Because azo monomers are highly hydrophobic, only the diblock copolymers with short azo segment were soluble in water which self-assembled into micellar particles. The effect of photo-induced *trans–cis* isomerization on lower critical solution temperature (LCST) and surface tension were studied. The LCST of the diblock copolymers increased upon irradiation by UV light due to the *cis* conformers being more hydrophilic. However, the *trans–cis* isomerization had only small effect on the critical micelle concentration (cmc) and γ_{cmc} of azo methacrylate block copolymers, due to the formation of compact core of the micelles. The formations of core-shell micelles were established from LLS and TEM studies. All the three azo methacrylate amphiphilic block copolymers formed hard core-shell micelles with relatively small R_h values of 31 nm for p($DMAEMA_{172}$-*b*-$BPHM_7$), 26 nm for p($DMAEMA_{172}$-*b*-$CPHM_7$) and 32 nm for p($DMAEMA_{172}$-*b*-$PPHM_9$). Whereas for the azo acrylate copolymer, p($DMAEMA_{172}$-*b*-$BPHA_6$), large micelles with $R_h \sim 78$ nm with loose core was formed.

Keywords: Water-soluble; Stimuli-responsive; Diblock copolymer

1. Introduction

Liquid crystalline (LC) polymers have attracted a great deal of interest due to their potential applications in optical switching, optical image storage and optical display [1,2]. Liquid crystalline polymers with azobenzene moieties in the side-chains are promising photonic and optical materials. This is because the azobenzene moiety can play the role of a mesogen and it is also photo-responsive. Azobenzene-containing (azo) polymers undergo *trans–cis* isomerization on photo-irradiation, where large changes occur in its size, shape and polarity. The *trans* form shows a LC phase due to its rod-like shape, while the *cis* form does not show LC phase due to its bent conformation [3–6]. Until recently, most of the azo LC copolymers reported are mainly synthesized by random copolymerization with azobenzene units present as side-chains [7,8]. There have been only few reports of azo block copolymers mainly due to the various constrains in the synthesis using free radical polymerization techniques [9,10]. The azo block copolymers have been observed to produce a variety of microstructures such as sphere, cylinder, lamellar morphologies, which could be tailored using precise control of the block lengths [11–13].

* Corresponding author. Tel.: +65 790 2811; fax: +65 896 9432.
E-mail address: lhgan@nie.edu.sg (L.H. Gan).

0032-3861/$ - see front matter © 2004 Elsevier Ltd. All rights reserved.
doi:10.1016/j.polymer.2004.11.009

Recently, ATRP technique has been employed for the synthesis of various azobenzene-containing polymers and copolymers. Photoactive thermoplastic elastomers of azobenzene-containing triblock copolymers prepared via ATRP was reported by Cui et al. [14] Branched azobenzene side-chain liquid-crystalline copolymers was prepared through self-condensing ATR copolymerization technique [15]. Self-condensing ATRP was also employed for the synthesis of hyperbranched azobenzene-containing polymers [16]. ATRP for the synthesis of multi-arm star azobenzene side-chain liquid crystalline copolymers with a hyperbranched core was reported by He et al. [17].

Water soluble amphiphilic azo polymers and azo-containing hydrogels have been reported for colon-specific drug delivery application [12,18–24]. In aqueous solutions, amphiphilic block polymers self-assemble into spherical micelles which are well suited for drug delivery and diagnostic systems [25,26]. Tian et al. [27] reported the synthesis of water soluble amphiphilic block copolymer of PEO-*b*-poly(11-(4-(4-butylphenylazo)phenoxy)undecyl methacrylate) via ATRP technique. An ABA type water soluble amphiphilic triblock copolymer containing azobenzene moieties and PEO segments was reported by He et al. [28] Both studies focused on the LC behavior of the block copolymers. In this paper, we report the synthesis of several diblock copolymers of azo acrylate and azo methacrylate monomers with 2-(dimethyl amino)ethyl methacrylate (DMAEMA) via ATRP. The diblock copolymers self-assemble into micelles and exhibit photo-responsive properties due to the azobenene unit and temperature- and pH-responsive properties due to the p(DMAEMA) segment.

2. Experimental

2.1. Materials

2-Dimethylaminoethyl methacrylate (DMAEMA) (98%, Merck) was dried over CaH_2 and distilled under reduced pressure. *p*-Toluenesulfonyl chloride (*p*-TsCl) (99%, Aldrich), ethyl 2-bromoisobutyrate (EBrIB) (98%, Aldrich), ethyl 2-bromopropionate (EBrP) (99%, Aldrich), copper(I) chloride (99.995%, Aldrich), copper(I) bromide (99.999%, Aldrich), 1,1,4,7,10,10-hexamethyltriethylenetetramine (HMTETA) (97%, Aldrich), and 1,1,4,7,7-pentamethyldiethylenetriamine (PMDETA) (99%, Aldrich) were used without further purification. All the solvents were freshly distilled before used. The azobenzene monomers, 6-[4-(4-buthoxyphenylazo)phenoxy]hexylacrylate (BPHA), 6-[4-phenylazo]phenoxy]hexylmethacrylate (PPHM), 6-[4-(4-buthoxyphenylazo)phenoxy]hexylmethacrylate (BPHM) and 6-[4-(4-cyanophenylazo)phenoxy]hexylmethacrylate (CPHM) were synthesized according to the procedure similar to the published method. [29].

2.2. Synthesis of azo methacrylate homopolymers

A typical ATRP experimental procedure for homopolymerization of PPHM is described as follows: To a 25 ml Schlenk reaction flask with a stirring bar, CuCl (12.02 mg, 0.121 mmol) and PPHM (0.4 g, 1.093 mmol) were introduced into the flask and sealed tightly with rubber septum. The flask was then evacuated and flushed with argon three times. Under an Ar atmosphere, deoxygenated anisole (4.0 ml) and HMTETA (33.0 μl, 0.121 mmol) were introduced using an Ar-washed syringe. The reaction mixture was degassed using three freeze–pump–thaw cycles. Finally, degassed EBrIB (8.91 μl, 0.061 mmol) was added through an Ar-washed syringe and the reaction was allowed to proceed on a thermostated oil bath at 85 °C. Samples were withdrawn periodically to determine the reaction kinetics. After the reaction was completed, it was stopped by diluting the reaction mixture with THF. The catalyst was removed by passing through a neutral alumina column. The filtrate was concentrated and the polymer was recovered by precipitating into large excess of methanol. The reprecipitation procedure was repeated three times. Finally, the polymer was filtered and dried in a vacuum oven at 30 °C for 24 h. Yield =74%, M_n=5900 and M_w/M_n=1.14. Homopolymers of BPHA, BPHM and CPHM were synthesized using the similar procedure.

2.3. Synthesis of p(DMAEMA)-Cl macroinitiator

The PDMAEMA with stable-Cl end groups was synthesized according to our previous work [30]. To a 25 ml Schlenk flask with a magnetic stirring bar, CuCl (0.031 g, 0.311 mmol) was added and the flask was evacuated and flushed with argon. Degassed methanol:water (3.6 ml methanol:1.4 ml water), HMTETA (0.085 ml, 0.311 mmol) and DMAEMA (10 ml, 59.34 mmol) were added to the Schlenk flask using Ar-washed syringe. The reaction mixture was stirred for 10 min after which it was degassed by three freeze–pump–thaw cycles. Before the final freeze–pump–thaw cycle, *p*-TsCl (0.0592 g, 0.311 mmol) was added. The reaction was allowed to proceed with constant stirring at room temperature. The reaction was stopped by diluting with THF and the mixture was passed through a basic alumina column. The filtrate was concentrated and the polymer was recovered by precipitating into excess of hexane. The reprecipitation procedure was carried out three times. The polymer was dried in a vacuum oven at 30 °C for 24 h. Yield: 74%. M_n=27,000, PDI=1.11. P(DMAEMA)-Cl with different molecular weight were obtained by varying the initiator:monomer molar ratio.

2.4. Synthesis of p(DMAEMA-b-azo methacrylates)

The synthesis of p($DMAEMA_{25}$-*b*-$PPHM_{19}$) is described as follows: to a 25 ml Schlenk flask, P(DMAEMA)-Cl

macroinitiator, (M_n = 4000, PDI = 1.11, 0.25 g, 0.061 mmol), CuCl (6.0 mg, 0.061 mmol) and PPHM (447 mg, 1.22 mmol) were introduced and the flask was subsequently evacuated and flushed with argon twice. The reaction mixture was dissolved in 3 ml of deoxygenated anisole. Three freeze–pump–thaw cycles were performed to remove the residual oxygen. Finally, deoxygenated HMTETA (17 μl, 0.061 mmol) was added using an Ar-purged syringe and the reaction flask was placed in a preheated oil bath maintained at 85 °C. The reaction was stopped by diluting with THF and the mixture was passed through a basic alumina column. The filtrate was concentrated and the polymer was recovered by precipitating into excess of hexane. The reprecipitation process was carried out for three times. The polymer was dried in a vacuum oven at 30 °C. Yield = 80%. M_n = 10,800, PDI = 1.12.

2.5. Characterizations

2.5.1. ^1H NMR spectroscopy

The ^{1}H NMR spectra of the block copolymers were measured using a Brüker DRX400 instrument in $CDCl_3$. The ^{1}H NMR spectrum of the block copolymer allows the molar composition to be determined from the relative intensity at 7.92 ppm (4H, Ar*H* from PPHM block) and 2.58 ppm (–NCH_2 of DMAEMA block).

2.5.2. Gel permeation chromatographic (GPC)

An Agilent 1100 series GPC system equipped with a LC pump, PLgel 5 μm MIXED-C column and RI detector was used to determine polymer molecular weights and molecular weight distributions. The column was calibrated with narrow molecular weight polystyrene standards. HPLC grade THF containing 1% triethylamine stabilized with BHT was used as the mobile phase. The flow rate was maintained at 1.0 ml/min.

2.5.3. UV–vis spectroscopy

UV–vis spectra were recorded using a Cary 50 Bio UV–visible spectrophotometer equipped with a digital temperature controller. The wavelength of 600 nm was used for the determination of LCST.

2.5.4. Surface tension

A KRUSS K 100 tensiometer equipped with a standard plate was used to determine the critical micelle concentration (cmc) values of amphiphilic diblock copolymers in aqueous solution. The polymer solution (0.45 mg/ml) was added gradually (in a dosage of 200 μl each) to a glass vessel containing 20 ml of distilled water at 20 °C. The surface tensions at different polymer concentrations were recorded.

2.5.5. Laser light scattering (LLS)

A Brookhaven BI-200SM goniometer system equipped with a 522 channel BI9000AT digital multiple τ correlator was used to perform dynamic light scattering experiments. The inverse Laplace transform of REPES in the Gendist software package was used to analyze the time correlation functions with probability of reject setting at 0.5. De-ionized water was used from Millipore Alpha-Q purification system equipped with a 0.22 micron filter. A 0.2 μm filter was used to remove dust prior to the light scattering experiments and the temperatures were controlled by a PolyScience water-bath. For static light scattering (SLS) studies, Zimm plot was used to analyze the experimental data. The refractive index increments,dn/dC, were measured by a BI-DNDC differential refractometer.

3. Results and discussion

3.1. Polymerizations

The synthetic route of azo acrylate and azo methacrylate monomers and that for the homopolymerisation via ATRP are outlined in Scheme 1(a) and (b), respectively. It was found that azo acrylates did not polymerize well via ATRP under the experimental conditions, yielding polymers of low and broad distribution of molecular weight. However, ATRP of three azo methacrylate monomers PPHM, BPHM and CPHM proceeded with reasonably well-controlled manner. The number-average molecular weight (M_n) of the p(PPHM$_{40}$) determined using GPC at different time intervals are shown in Fig. 1. The GPC traces shifts towards lower elution time showing the molar mass of the polymer increases with time. Relatively low polydispersity indexes (PDI) (1.12–1.16) were obtained for all three monomers PPHM, BPHM and CPHM. The kinetic plots of ln([M]$_0$/[M]) versus %conversion were all linear, up to ~50% conversion, indicating the controlled/'living' characteristics of polymerizations using the EBrIB/CuCl/HMTETA ATRP system.

Diblock copolymers were prepared via ATRP using p(DMAEMA)Cl macroinitiators of various chain length.

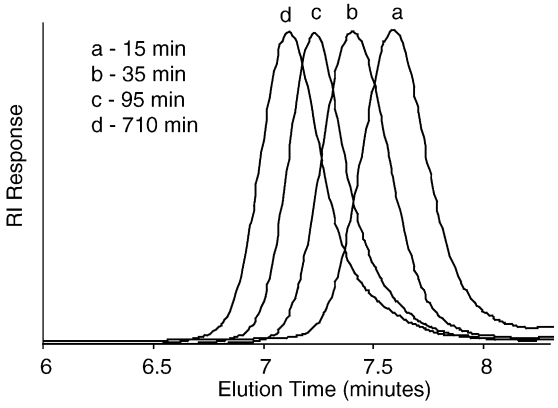

Fig. 1. GPC traces of the p(PPHM$_{40}$) homopolymer at different time intervals.

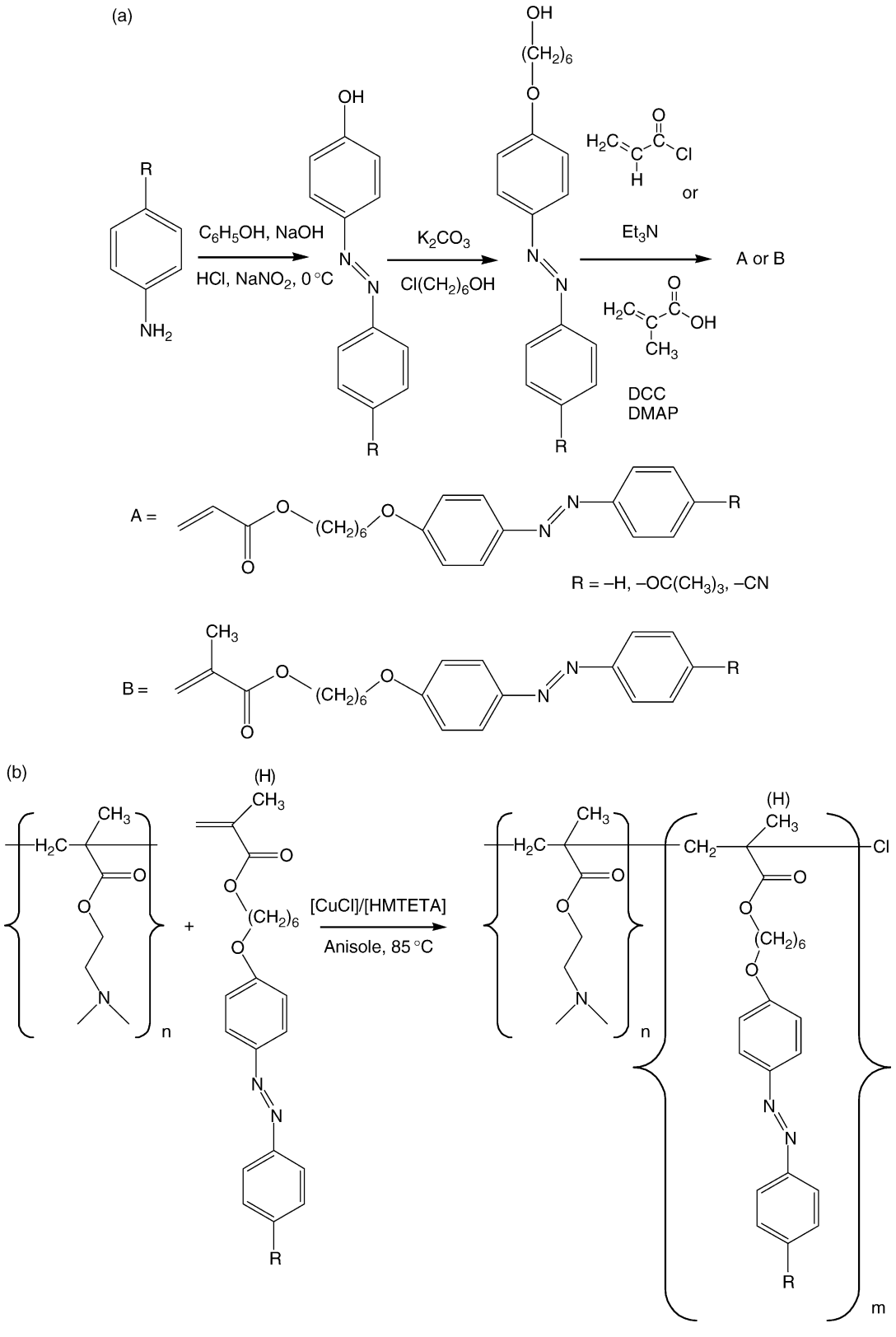
(a)
C6H5OH, NaOH
HCl, NaNO2, 0 °C
K2CO3
Cl(CH2)6OH
Et3N
or
A or B
DCC
DMAP
A =
B =
R = –H, –OC(CH3)3, –CN
(b)
[CuCl]/[HMTETA]
Anisole, 85 °C

Scheme 1.

Table 1
Homopolymers of azo methacrylates and azo copolymers of DMAEMA

Samples	$[M]_0/[I]_0$	Time (h)	M_n (GPC)	M_n (NMR)	M_n (Cal)	PDI
p($PPHM_{16}$)	18	23	5900	–	6600	1.14
p($PPHM_{40}$)	50	22	14,500	–	18,300	1.15
p($BPHM_{25}$)	50	24	11,100	–	21,900	1.16
p($CPHM_{16}$)	50	24	6300	–	19,600	1.1
p($DMAEMA_{25}$-*b*-$PPHM_{19}$)	20	6	10,800	11,000	11,300	1.12
p($DMAEMA_{94}$-*b*-$PPHM_{19}$)	30	5	21,800	22,700	25,700	1.14
p($DMAEMA_{172}$-*b*-$PPHM_9$)	30	24	30,300	29,900	37,900	1.14
p($DMAEMA_{172}$-*b*-$CPHM_7$)	30	5	29,900	29,100	38,700	1.20
p($DMAEMA_{172}$-*b*-$BPHM_7$)	20	5	30,000	29,600	35,800	1.13
p($DMAEMA_{46}$-*b*-$BPHM_{11}$)	25	7	12,000	12,000	18,300	1.15
p($DMAEMA_{172}$-*b*-$BPHA_6$)	15	24	29,500	29,100	33,400	1.14

Again, azo acrylate monomers were found to be unreactive. Only a small number of the monomer units (<10) were incorporated into the copolymers. On the other hand, well-controlled copolymerizations of azo methacylate monomers were observed. The results are summarized in Table 1. The GPC profile for the p($DMAEMA_{94}$-*b*-$PPHM_{19}$) at different polymerization time intervals using p(DMAEMA) macroinitiator, shows the smooth increment of molar masses (Fig. 2). Fig. 3 shows the plots of M_n and PDI as a function of % conversion for PPHM copolymerization. The kinetic plot of $\ln([M]_0/[M])$ versus time is linear and the apparent rate constant k_{app} value can be calculated using Eq. (1) for living polymerizations proposed by Matyjaszewski et al. [31]

$$\ln\left(\frac{[M]_0}{[M]}\right) = k_p K_{eq} \frac{[RX][Cu(I)]}{[Cu(II)]} t = k_{app} t \quad (1)$$

It was found that $k_{app} = 0.0078\ min^{-1}$ for the extension of PPHM in the copolymer is practically identical to the value ($k_{app} = 0.0077\ min^{-1}$) for homopolymerization of PPHM. Almost complete monomer conversion was achieved when the chain length of the macroinitiator was relatively short. The M_n agrees well with the targeted values. However, it was found that p(DMAEMA) macroinitiator with longer chain length did not yield full conversion of azo methacrylate monomers. Because of the long chain length, the active chain ends are likely to be embedded due to chain folding, causing the propagation rate to decrease greatly. Steric hindrance caused by the highly bulky azo methacrylate monomers, which could be more acute for longer chain molecules, might also be a factor for the poor conversion.

The molecular weights (M_n) and the composition of the block copolymers were also determined by ^1H NMR spectra (Fig. 4) using following equation:

$$MWM + \frac{MWM \times 366 \times xI_2}{157 \times 2 \times I_1} \quad (2)$$

where MWM is the M_n of the macroinitiator, the units 366 and 157 refer to molar mass of PPHM and DMAEMA monomers, I_1 and I_2 are the integration values at 2.58 ppm (2H, –NCH_2– of DMAEMA segments) and 7.92 ppm (4H,

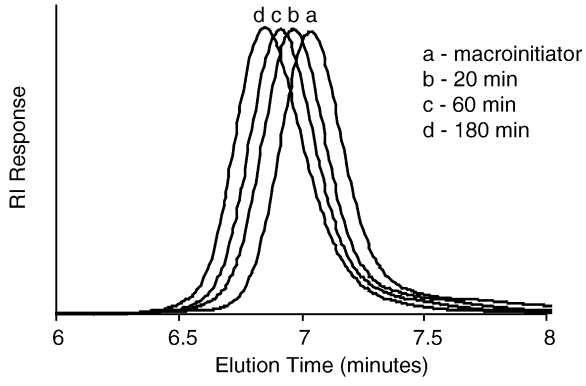

Fig. 2. GPC traces of the p($DMAEMA_{94}$-*b*-$PPHM_{19}$) at different time intervals.

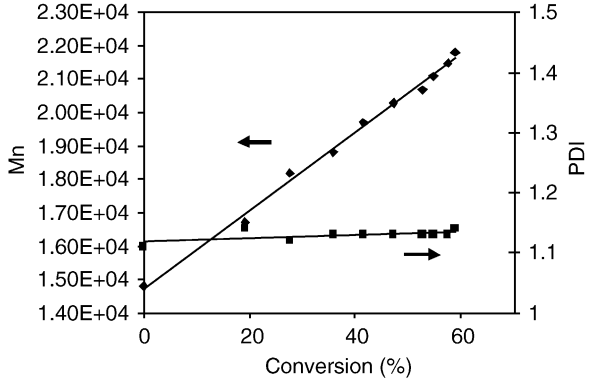

Fig. 3. Molecular weight (M_n) and polydispersity index (PDI) as a function of monomer conversion for the p($DMAEMA_{94}$-*b*-$PPHM_{19}$).

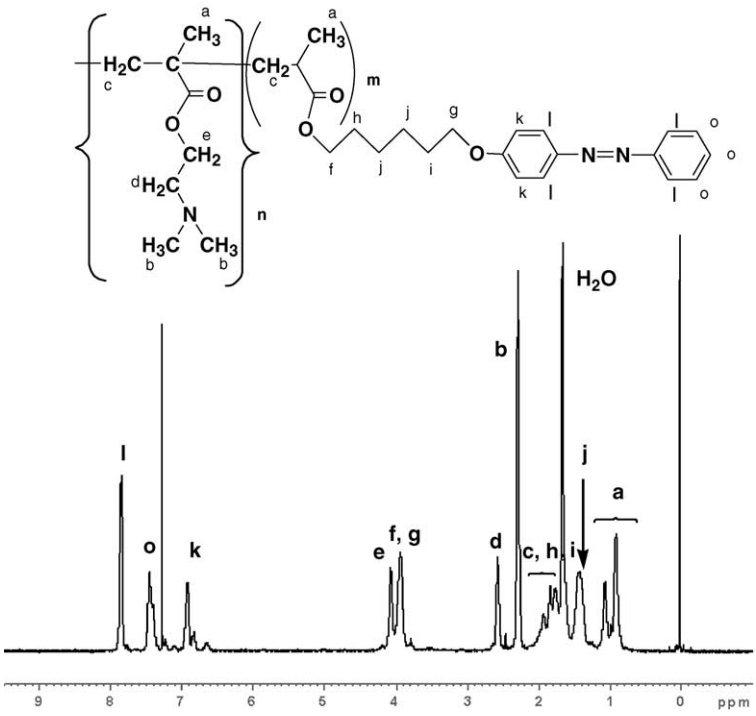

Fig. 4. ^{1}H NMR spectrum of the p(DMAEMA$_{25}$-*b*-PPHM$_{19}$) in $CDCl_3$.

Ar*H* of PPHM segments) respectively. The molar mass of the diblock copolymer calculated from ^{1}H NMR are in good agreement with the M_n values determined using GPC.

3.2. Photoisomerization: effect on LCST and surface tension

Photoisomerizations of diblock copolymers in aqueous solution were investigated. Upon irradiation at 366 nm, the absorbance at 445 nm, corresponding to the n–π* transition (*cis* state) increased, while that at 346 nm corresponding to the π–π* transition (*trans* state) decreased with irradiation time. For the aqueous solution of p(DMAEMA$_{94}$-*b*-PPHM$_{19}$) (0.045 wt%), the decrease in absorbance at 346 nm reached the photostationary value after 5 min of irradiation (Fig. 5). The solution was then kept in the dark. As the *cis* isomer is thermodynamically less stable, it spontaneously isomerizes back to the *trans* form due to thermal energy. The reverse *cis–trans* isomerizations at different time intervals are also shown in Fig. 5. The results establish the fact that the reverse thermal *cis–trans* isomerization is a slow process.

The *%T* changes as a function of temperature of p(DMAEMA$_{172}$-*b*-PPHM$_9$) aqueous solutions measured at 600 nm are shown in Fig. 6. p(DMAEMA) and its block copolymers are thermal-sensitive polymers exhibiting LCST phenomenon [32–34]. The aqueous solution of p(DMAEMA$_{172}$-*b*-PPHM$_9$) showed the LCST at 41 °C. After irradiation the LCST of p(DMAEMA$_{172}$-*b*-PPHM$_9$) increased to 44 °C as the *cis*-conformer is more hydrophilic than the *trans*-conformer. The LCST values were

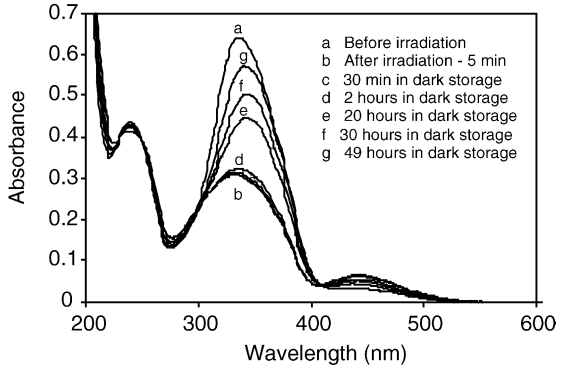

Fig. 5. UV–vis spectra of 0.045 wt% aqueous solution of p(DMAEMA$_{94}$-*b*-PPHM$_{19}$) before and after irradiation at 366 nm and various storage time at 25 °C.

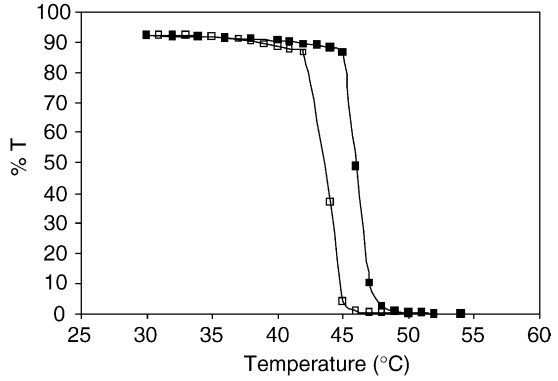

Fig. 6. %T at 600 nm of 0.7 wt% aqueous solutions p(DMAEMA$_{172}$-*b*-PPHM$_9$) before (□) and after (■) irradiation at different temperature.

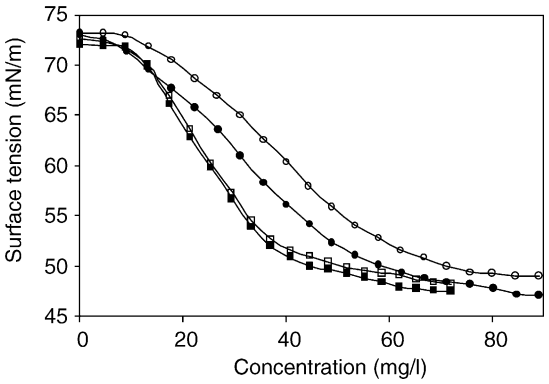

Fig. 7. Surface tension versus concentration of the aqueous solutions of p(DMAEMA$_{94}$-*b*-PPHM$_{19}$) (○: before; ●: after) and p(DMAEMA$_{172}$-*b*-PPHM$_9$) (□: before; ■: after) before and after irradiation at 366 nm.

determined from the minimum of the first derivative of $\%T$ versus temperature curves.

In aqueous solutions, diblock copolymers of DMAEMA and azo monomers readily form micelles due to their amphiphilic behavior. The effect of photo-irradiation on micellization was studied. It was found that the surface tension versus concentration plots of p(DMAEMA$_{172}$-*b*-PPHM$_9$) changed only slightly after irradiation, although it dropped off to a slightly lower value, as shown in Fig. 7. Apparently, the different *cis* and *trans* conformations of the azobenzene has little effect on the micelle formation for this sample, partly due to the extremely short segment of PPHM compared to that of DMAEMA. The effect was more pronounced however, for p(DMAEMA$_{94}$-*b*-PPHM$_{19}$) which has a much higher PPHM/DMAEMA block ratio (Fig. 7). The equilibrium surface tension (γ_{cmc}) is clearly lower after irradiation (also shown in Fig. 7). However, the cmc values were again nearly the same for the *cis* and *trans* conformers. The above observation is in qualitative agreement with a

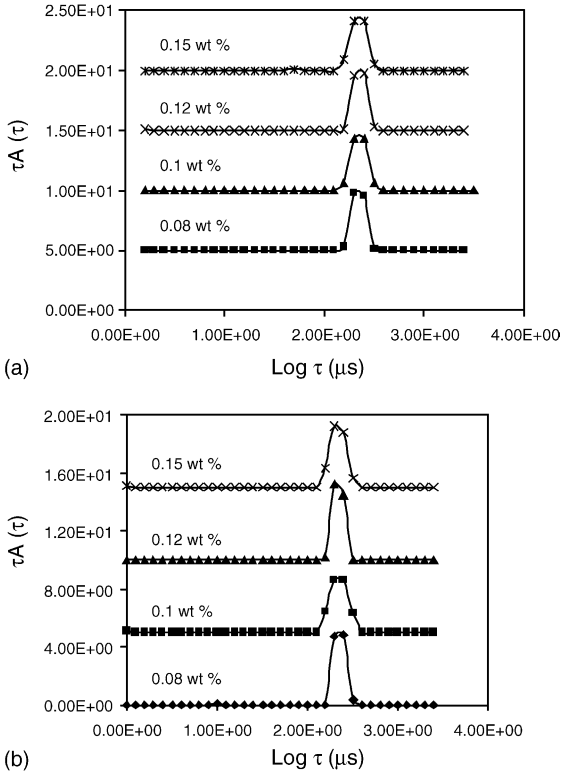

Fig. 9. Decay time distribution functions of p(DMAEMA$_{172}$-*b*-PPHM$_9$) in aqueous solutions with different concentrations measured for 90° at 25 °C: (a) before irradiation (b) after irradiation at 366 nm.

recent report by Shang et al. [35] using a series of small surfactants with polar di(ethylene oxide) headgroup connected to (4-butylazobenzene)ether designated as C$_4$-AzoOC$_n$E$_2$ ($n=2$, 4, 6, 8). It was reported that for surfactants with shorter spacer lengths ($n=2$, 4 and 6), the cmc and γ_{cmc} are larger for all the *cis* conformers compared to the *trans* forms. However, anomalous behavior were

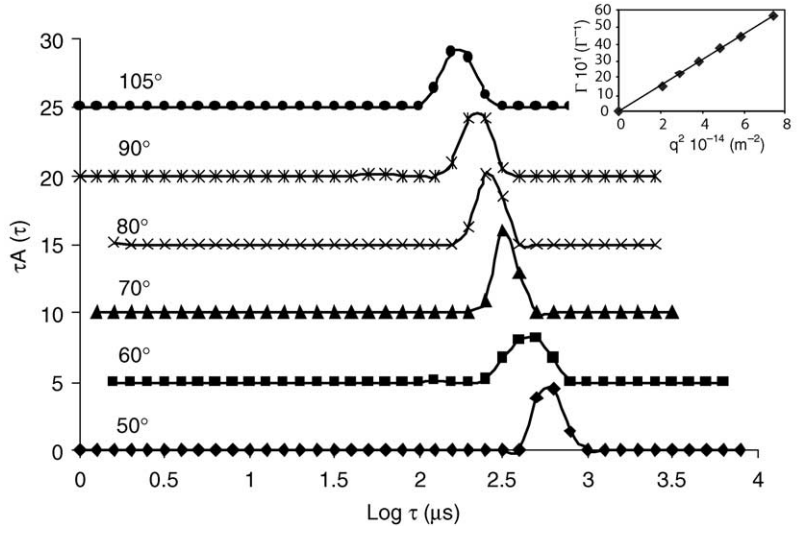

Fig. 8. Decay time distribution functions of 0.15 wt% aqueous solutions of p(DMAEMA$_{172}$-*b*-PPHM$_9$) for different angles at 25 °C. Inset of the figure represents Γ versus q^2.

observed when the spacer length increased to $n=8$. It was found that the cmc values for the two conformers were nearly the same, with only slightly higher value for the *cis* conformer. For γ_{cmc}, the trend actually reversed, where a smaller γ_{cmc} for the *cis* conformation was observed.

3.3. Laser light scattering studies

The decay time distribution functions of p(DMAEMA$_{172}$-*b*-PPHM$_9$) solution at different scattering angles are shown in Fig. 8. In all cases, only one decay mode is evident in the relaxation time distribution function, and the distribution function shifts to lower relaxation time with increasing scattering angles. The inset of the Fig. 8 shows that the decay rates Γ, inverse of the relaxation times τ, are q^2 dependence, suggesting the decay mode is caused by the translational diffusion of the particles in solutions. This implies only one type of particle was present in the solution. Fig. 9(a) shows the relaxation time distribution functions with different concentrations for p(DMAEMA$_{172}$-*b*-PPHM$_9$) before irradiation where the azobenzene moiety exists mostly in the *trans* conformation. The relaxation time distribution or translational diffusion coefficients are independent of the concentrations, implying that aggregates are produced according to the closed-model association mechanism, which predicts concentration-independent R_h. The solutions were examined again after irradiation at 366 nm, this time using a 621 nm laser light source. The decay time distribution functions with different concentrations for p(DMAEMA$_{172}$-*b*-PPHM$_9$) after irradiation are shown in Fig. 9(b). It was found that the decay time was again concentration-independent, suggesting R_h values of the particles were not affected by the *trans–cis* isomerisation. These results corroborate the surface tension data. Apparently the hydrophilic effect induced by the *cis* conformation was not able to dominate the hydrophobic effect.

For dynamic light scattering, R_h was determined from the Stokes–Einstein Eq. (2)

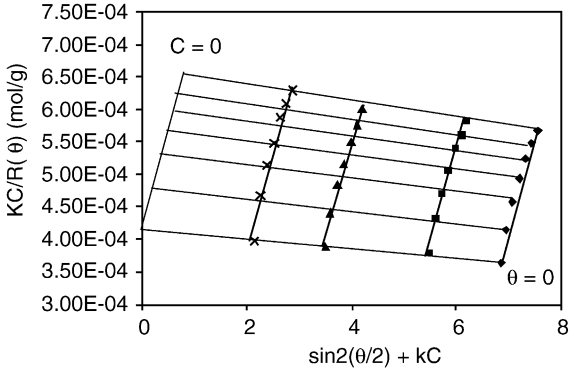

Fig. 10. Zimm plot of p(DMAEMA$_{172}$-*b*-BPHA$_6$) in aqueous solution at 25 °C using the concentration range from 0.3 to 1 mg/ml.

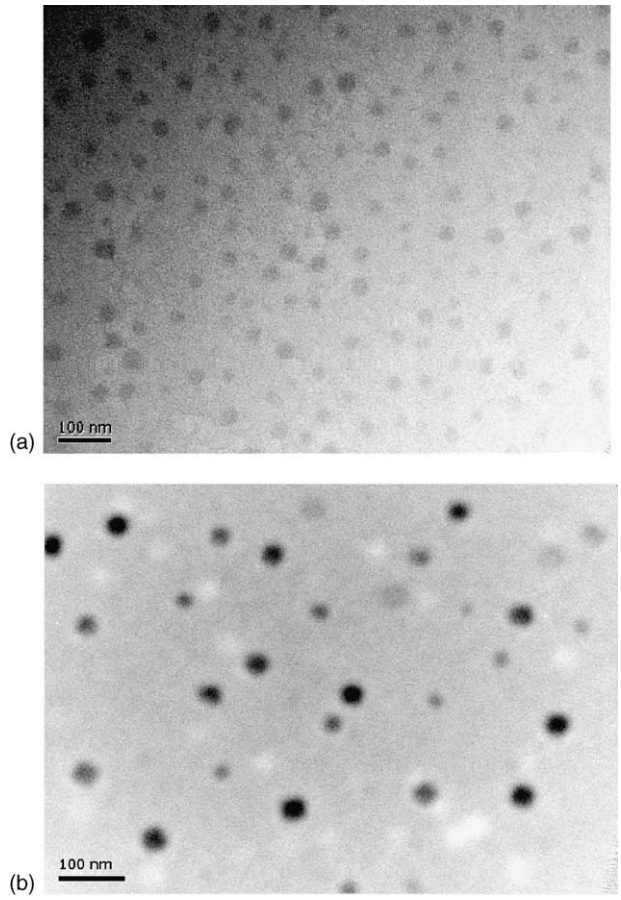

Fig. 11. TEM micrographs of aggregates of (a) p(DMAEMA$_{172}$-*b*-BPHM$_7$) and (b) p(DMAEMA$_{172}$-*b*-BPHA$_6$).

$$R_h = \frac{kT}{6\pi\eta_0 D_0} \tag{3}$$

where η_0 is the solvent viscosity, T the absolute temperature, D_0 the translational diffusion coefficient at infinite dilution, and k, the Boltzmann constant. For very dilute solutions, D can be approximated to D_0.

Interestingly, it was found that the DMAEMA diblock copolymers of azo acrylate and azo methacrylate aggregate quite differently. Diblock copolymers of almost equal block lengths, i.e. p(DMAEMA$_{172}$-*b*-BPHA$_6$) and p(DMAEMA$_{172}$-*b*-BPHM$_7$) were synthesized and studied. It was found that p(DMAEMA$_{172}$-*b*-BPHA$_6$) aggregates into particles of bigger size ($R_h \sim 78$ nm) than the aggregates of p(DMAEMA$_{172}$-*b*-BPHM$_7$) which has $R_h =$ 31 nm. The azo methacrylates are more hydrophobic than the azo acrylates. Thus azo methacylate block copolymers form aggregates with more compact cores, contributed to the lower R_h values. The difference in the aggregate size could also be partly due to the difference in T_g values of the two azo polymer blocks. Methacrylate based polymers possess higher T_g than that of the corresponding acrylate, i.e. $T_g \sim 85$–105 °C for poly(methyl methacrylate) [36] vis-a-vis $T_g \sim 9$ °C for poly(methyl acrylate). The results

suggest that p(DMAEMA$_{172}$-*b*-BPHM$_7$) forms hard core-shell micelles with BPHM$_7$ forming the core and DMAEMA$_{172}$ the corona. This is reasonable, considering the length of the fully extended corona DMAEMA block is ~40 nm. The R_h values for the aggregates of the other two azo methacrylates, p(DMAEMA$_{172}$-*b*-CPHM$_7$) and p(DMAEMA$_{172}$-*b*-PPHM$_9$) were found to be 26 and 32 nm respectively, showing the substituents on the azobenzene unit has relatively small effect on the size of the core.

For p(DMAEMA$_{172}$-*b*-BPHA$_6$), the larger R_h value suggests that the micelles are formed with loosely packed core. This is confirmed from the static light scattering (SLS) studies. The Zimm plot for p(DMAEMA$_{172}$-*b*-BPHA$_6$) solution with concentration ranging from 0.03 to 0.1 wt% is shown in Fig. 10. The radius of gyration (R_g) and the weight-average molecular weight (M_w) of the aggregates were determined to be 78 nm and 6.1×10^6 g/ml respectively. The aggregation number (N_{agg}) is 183. The $R_g/R_h=0.92$ is in line with the suggestion that the micelles formed has a relatively loose core. Hard core-shell spherical micelles are typically with $R_g/R_h\sim0.77$.

The micellar aggregates of p(DMAEMA$_{172}$-*b*-BPHM$_7$) and p(DMAEMA$_{172}$-*b*-BPHA$_6$) were also observed by TEM (Fig. 11(a) and (b)). Spherical particles with smooth surface and fairly uniform size can clearly be seen for both the diblock copolymers. However, the sizes of the particles, with diameters ~30 nm for p(DMAEMA$_{172}$-*b*-BPHM$_7$) and ~50 nm for p(DMAEMA$_{172}$-*b*-BPHA$_6$) observed in the TEM are smaller than those obtained from the DLS studies. The smaller particle size observed from the TEM micrographs could be due to the sample preparation where the particles could have shrunk upon drying.

4. Conclusions

New water soluble stimuli-responsive diblock copolymers of DMAEMA with azo acrylate and azo methacrylate monomers were successfully synthesized via ATRP. The aqueous solutions of the diblock copolymers show LCST phenomenon. The LCST of the diblock copolymers increased upon irradiation by UV light due to *trans–cis* isomerization as the *cis* conformers are more hydrophilic. The photo-induced *trans–cis* isomerization has only small effect on the cmc and γ_{cmc} of azo methacrylate block copolymers due to the formation of compact core as a result of high T_g. The formations of core-shell micelles were established from LLS and TEM studies. The R_h values of the three azo methacrylate block copolymers, 31 nm for p(DMAEMA$_{172}$-*b*-BPHM$_7$), 26 nm for p(DMAEMA$_{172}$-*b*-CPHM$_7$) and 32 nm for p(DMAEMA$_{172}$-*b*-PPHM$_9$) are much smaller than the 78 nm for the azo acrylate copolymer, p(DMAEMA$_{172}$-*b*-BPHA$_6$).

Acknowledgements

This research is funded by the academic fund, National Institute of Education (NIE), Nanyang Technological University, RI 9/03. SLS thanks NIE for the postgraduate research scholarship.

Appendix. Supplementary Material

Supplementary data associated with this article can be found, in the online version, at doi:10.1016/j.polymer.2004.11.009.

References

[1] Holme NCR, Ramanujam PS, Hvilsted S. Opt Lett 1996;21:902.
[2] Sekkat Z, Wood J, Aust EF, Knoll W, Volksen W, Miller RD. J Opt Soc Am B 1996;13:1713.
[3] Stumpe J, Muller L, Kreisig D, Hauck G, Koswig HD, Ruhmann R, Rubner J. Makromol Chem, Rapid Commun 1991;12:81.
[4] Anderle K, Wendorff JH. Mol Cryst Liq Cryst 1994;243:51.
[5] Hvilsted S, Andruzzi F, Kulinna C, Siesler HW, Ramanujam PS. Macromolecules 1995;28:2172.
[6] Wang C, Fei H, Qiu Y, Yang Y, We Z, Tian Y, Chen Y, Zhao Y. Appl Phys Lett 1999;74:19.
[7] Natansohn A, Rochon P. Chem Rev 2002;102:4139.
[8] Viswanathan NK, Kim DY, Bian S, Williams J, Liu W, Li L, Samuelson L, Kumar J, Tripathy SK. J Mater Chem 1999;9:1941.
[9] Natansohn A, Rochon P, Gosselin J, Xie S. Macromolecules 1992;25:2268.
[10] Krueger H, Wolff D, Aschuppe V. Acta Polym 1992;43:283.
[11] Mao G, Ober CK. Abstract of the NERM (Northeast Regional Meeting of the American Chemical Society), Rochester, NY, 1995. Wasington, DC: ACS; 1995. p. 198.
[12] Mao G, Wang J, Clingman SR, Ober CK, Chen JT, Thomas EL. Macromolecules 1997;30:2556.
[13] Schneider A, Zanna JJ, Yamada M, Finkelmann H, Thomann R. Macromolecules 2000;33:649.
[14] Cui L, Tong X, Yan XH, Liu GJ, Zhao Y. Macromolecules 2004;37:7097.
[15] He XH, Yan DY. Macromol Rapid Commun 2004;25:949.
[16] Jin M, Lu R, Bao CY, Xu TH, Zhao YY. Polymer 2004;45:1125.
[17] He XH, Yan DY, Mai YY. Eur Polym J 2004;40:1759.
[18] Yamaoka T, Makita Y, Sasatani H, Kim SI, Kimura Y. J Control Release 2000;66:187.
[19] Maris B, Verheyden L, Van Reeth K, Samyn C, Augustijns P, Kinget R, Van den Mooter G. Int J Pharm 2001;213:143.
[20] Saffran M, Kumar G, Savariar C, Burnham JC, Williams F, Neckers DC. Science 1986;233:1081.
[21] Brondsted H, Kopecek J. Biomaterials 1991;12:584.
[22] Brondsted H, Kopecek J. Pharm Res 1992;9:1540.
[23] Mooter GV, Samyn C, Kinget R. Int J Pharm 1994;111:127.
[24] Mooter GV, Samyn C, Kinget R. Pharm Res 1995;12:244–7.
[25] Kwon GS, Okano T. Adv Drug Deliv Rev 1996;21:107.
[26] Trubetskoy VS. Adv Drug Deliv Rev 1999;37:81.
[27] Tian Y, Watanabe K, Kong X, Abe J, Iyoda T. Macromolecules 2002;35:3739.
[28] He X, Zhang H, Yan D, Wang X. J Polym Sci, Part A: Polym Chem 2003;41:2854.
[29] Ringsdorf H, Schmidt HW. Makromol Chem 1984;185:1327.

[30] Mao BW, Gan LH, Gan YY, Li XS, Ravi P, Tam KC. J Polym Sci, Part A: Polym Chem 2004;42:5161.
[31] Matyzaszweski K, Patten TE, Xia J. J Am Chem Soc 1997;119:674.
[32] Weaver JVM, Armes SP, Bütün V. Chem Commun 2002;2122.
[33] Lowe AB, Billingham NC, Armes SP. Macromolecules 1998;31: 5991.
[34] Liu S, Weaver JVM, Tang Y, Billingham NC, Armes SP, Tribe K. Macromolecules 2002;35:6121.
[35] Shang TG, Smaith KA, Hatton AT. Langmuir 2003;19:10764.
[36] Callister Jr WD. Materials science and engineering: an introduction. 3rd ed. New York: Wiley; 1994. p. 769.